Theoretical study on thermochemistry of solvated lithium-cation with propylene carbonate

**Haruhiko Ohtani · Yasukazu Hirao ·
Akihiro Ito · Kazuyoshi Tanaka · Osamu Hatozaki**

Abstract We report the theoretical analysis results of thermochemical properties of solvated Li^+ ion in propylene carbonate (PC), which is one of the most popular solvents used in the lithium-ion battery composite. In the theoretical calculation, we employed the density functional theory method with the 6-31G basis set using the Gaussian03 package. It has been made clear that the solvation with four PC molecules around a Li^+ ion is most favorable. Detailed results of the conventional quantum chemical analyses for these materials will also be presented. Thermochemical properties such as the standard (that is at 298.15 K and 101325 Pa) enthalpy, entropy, and Gibbs energy changes upon the formation of Li^+ complexes solvated with PC molecules have been numerated and discussed. Furthermore, we will afford the features of desolvation of the solvated Li^+ ion complexes when they interact with the carbon electrode modeled by ovalene molecules.

Keywords Lithium-ion battery · Li^+ ion · Solvation · Carbon electrode · Desolvation · DFT calculation

H. Ohtani · Y. Hirao · A. Ito · K. Tanaka (✉)
Department of Molecular Engineering, Graduate School
of Engineering, Kyoto University, Nishikyo-ku,
Kyoto 615-8510, Japan
e-mail: a51053@sakura.kudpc.kyoto-u.ac.jp

O. Hatozaki
Subaru Technical Research Center, Fuji Heavy Industries Ltd.,
9-6-3-Chome, Osawa, Mitaka-shi, Tokyo 181-8577, Japan

Present Address:
Y. Hirao
Department of Chemistry, Graduate School of Science,
Osaka University, 1-1 Machikaneyamacho, Toyonaka,
Osaka 560-0043, Japan

Introduction

Lithium-ion battery is one of the most important electricity-storage devices applicable to a wide range of electronic devices as well as possibly to electric vehicles. In lithium-ion batteries, Li^+ ions dissolved in an electrolyte solution move back and forth between the negative and positive electrodes during the charging–discharging processes. It is important, hence, to investigate behavior of Li^+ ions in the electrolyte to fully understand the microscopic processes in the lithium-ion batteries. The negative electrode often employs the carbon material since it shows the high-performance behavior with excellent energy density and charge–discharge characteristics [1].

In the charging process of the lithium-ion battery, Li^+ ions migrate from the electrolyte solution phase into the negative electrode and then doped (or intercalated) inside the electrode. In this sense, clarification of the behavior of Li^+ ions when they move from the solution to the electrode is of much importance for understanding the microscopic aspects of the redox reaction occurring in the battery.

It is considered that a Li^+ ion in the electrolyte solution consisting of organic solvent and supporting electrolyte is surrounded with a certain numbers of solvent molecules, generally referred to as solvation. There have been attempts to estimate the solvation number for Li^+–organic solvent complexes by Raman intensity study [2, 3]. The solvation numbers for Li^+ ion has also theoretically been examined with respect to ethylene carbonate (EC) and methylethyl carbonate (MEC) molecules as the solvent using the Hartree–Fock method [4]. From these experimental and theoretical studies, the solvation number of Li^+–EC complex has been estimated as four [2, 4]. Solvation of Li^+ ion with the ordinary organic solvent molecules like acetone, acetonitrile, and so on has also been examined [5, 6].

On the other hand, propylene carbonate (PC; see Fig. 1a) is one of the most popular solvents widely used in the lithium-ion battery composite and has liquid phase in a wide temperature range, i.e., from 218.15 to 513.15 K [7]. But not enough studies for the Li$^+$–PC solvated complex have been hitherto carried out to the authors' knowledge. Hence, in this study, quantum chemical [density functional theory (DFT) method] calculation is undertaken toward clarification of the electronic structures of the solvated Li$^+$ ion when PC is used as the solvent (see Fig. 1b). Emphasis is made to clarify the most appropriate number of the PC molecules solvated to a Li$^+$ ion. Besides the conventional quantum chemical analysis on the electronic structures, reaction parameters such as the standard (that is at 298.15 K and 101325 Pa) enthalpy, entropy, and Gibbs energy changes upon the solvation are estimated to discuss the thermochemical behavior of the solvated Li$^+$ ion complexes.

Moreover, we also examine desolvation of the solvated complex when it is adsorbed onto the carbon electrode models set up using a certain condensed aromatic hydrocarbon (ovalene) molecules (see Figs. 1c, d).

Method of calculation

Quantum chemical calculations were performed based on the DFT method within the hybrid HF/DF (B3LYP) framework. For all the solvated Li$^+$ ion with PC molecules were carried out geometry optimizations using the 6-31G basis set. The atom–atom overlap-weighted bond-order indices between Li$^+$ and connected O atoms of PC molecules are analyzed based on the natural atomic orbitals (NAOs) [8].

For these solvated species were estimated thermochemical parameters such as the change in the standard enthalpy, entropy, and Gibbs energy upon the solvation
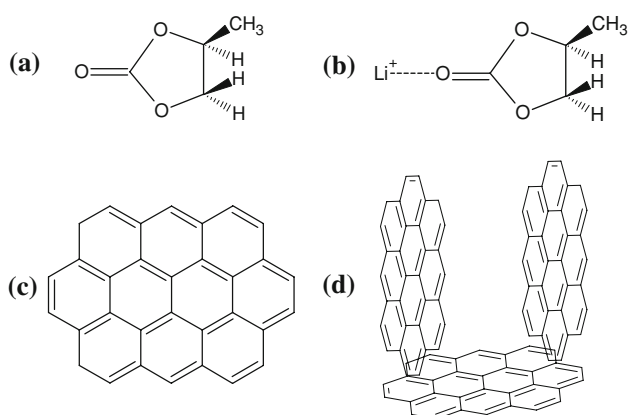
with the optional procedure including calculations of the molecular vibration frequencies, molecular rotation energies, etc., and then the partition functions. The Gaussian03 package [9] was employed for all the DFT calculations as well as the numeration of the thermochemical data. Details about the thermochemical calculations are abbreviated for simplicity, but the information can be obtained in the web (http://www.gaussian.com/g_whitepap/thermo/thermo.pdf).

Furthermore, for lithium-ion batteries, analysis of the interaction between Li$^+$ ion and the electrode is quite interesting. In this study, the interaction between a carbon electrode model and solvated Li$^+$-ion complex is examined. As to this analysis, a possible process is as follows: (i) a solvated Li$^+$-ion complex is at first adsorbed on a carbon electrode surface, (ii) desolvated at second, and then (iii) Li$^+$ cation is diffused inside the electrode material as a dopant. Here, we take an amorphous carbon as the electrode rather than rigid graphite surface.

An ovalene molecule optimized with the B3LYP 6-31G basis set (Fig. 2a) was employed to set up three kinds of the carbon electrode models as shown in Fig. 2: (a) an ovalene molecule itself as a simple surface wall, (b) a parallel walls with the distance of 600 pm, and (c) a micropore model consisting of three ovalene molecules. For these surface models, the molecular structure of ovalene(s) as well as the distance between the two parallel walls and micropores was kept rigid when the solvated Li$^+$ complex is adsorbed. For the supermolecular systems, including the Li$^+$ complex and the parallel wall model or the micropore model were utilized the 3-21G basis set for the economical reason.

The SCF threshold value was set 0.4184 kJ mol^{-1} for all the DFT calculations. It is necessary that attention should be taken care for the basis-set superposition error (BSSE) effect when the molecular complex as in this study is dealt with especially for the economical basis set. Examination for the present Li$^+$–PC$_1$ solvated complex, for instance, the B3LYP/6-31G basis set gave the energy error of 0.0014% (14.598 kJ mol^{-1} vs. the total electronic energy -1021214.365 kJ mol^{-1}) and 3-21G of 0.0047% (48.204 kJ mol^{-1} vs. the total electronic energy -1015956.196 kJ mol^{-1}). Thus, the BSSE is expected to be not serious here, and it is disregarded throughout this study. The BSSE correction has similarly been neglected in the calculation for Ag$^+$ ion coordinated to polypyridine ligands [10].

Results and discussion

Geometrical optimization

Configurations of Li$^+$–PC$_x$ solvated complexes ($x = 1$–6) obtained by the geometrical optimizations are shown in

Fig. 1 Schematic drawing of molecular structures of **a** propylene carbonate, **b** Li$^+$–PC complex, **c** ovalene, and **d** micropore model constructed by ovalene molecules
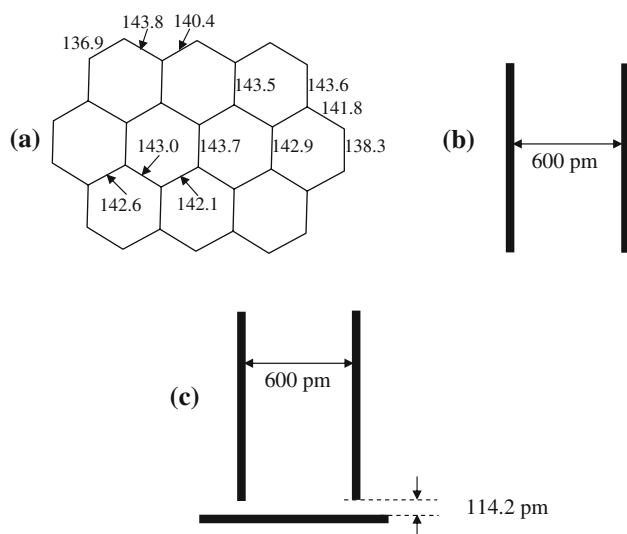
Fig. 2 **a** Molecular structure of ovalene with the optimized C–C bond lengths (in pm). The C–H bond lengths (108.6–108.7 pm) and bond angles are abbreviated. **b**, **c** Models for the carbon electrodes: **b** two-wall model and **c** micropore model consisting of ovalene molecules, whose planes are shown by *thick bars*

Fig. 3. It is seen that Li$^+$ ion is surrounded with carbonyl O atoms of PC molecules. It is shown in Table 1 that the interatomic distances between Li and the carbonyl O are equivalent in each Li$^+$–PC$_x$ ($x = 2$–4) (see also Fig. 3b–d). On the other hand, two PC molecules tend to be liberated from the solvated complex in Li$^+$–PC$_5$ and, moreover, the

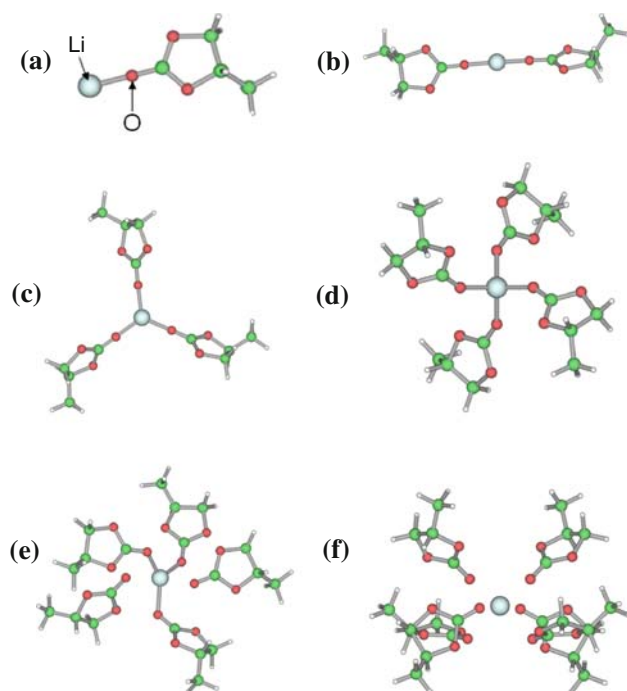**Fig. 3** Structures of solvated Li$^+$–PC$_x$ complexes obtained by the calculation; **a–f** correspond to $x = 1$, 2, 3, 4, 5, and 6, respectively. Li$^+$ is in the center position

solvation complex itself is almost decomposed in Li$^+$–PC$_6$; although, the configurations in Fig. 3e and f are of the energy-minimum ones. These tendencies are reflected in the difference of average and maximum distances of Li–O in these complex species in Table 1.

Electronic structure of Li

Positive charge of the Li$^+$ ion decreases with increase in numbers of solvated PC molecules as seen in Table 1. This positive charge flows into the carbonyl O atoms, suggesting the charge relaxation of Li$^+$ upon the solvation. The bond-order analyses with respect to Li–O bond listed in Table 2 obviously suggest that two and the all PC molecules are leaving from Li$^+$ ion, respectively, in Li$^+$–PC$_5$ and Li$^+$–PC$_6$ complexes.

All these results strongly suggest that the maximum numbers of PC molecules that can solvate a Li$^+$ ion is *four*. Hence formation of the Li$^+$–PC$_4$ complex is expected in PC solvent. This situation is similar to the solvation number in different solvent species such as EC previously studied [2, 4]. It is obvious that the solvation number of Li$^+$ depends on the steric features of the corresponding organic solvent. For instance, the favorable solvation number has been reported to be three in acetone and tetrahydrofuran and two in diethyl-ether [5]. On the other hand, it has been suggested that less bulky solvent molecule like acetonitrile would make even six coordination to a Li$^+$ ion [6].

Thermochemical data

The calculated values of changes in the standard enthalpy, entropy, and Gibbs energy upon the solvation are listed in Table 3. These values are defined as the difference in those for the solvated complex and entirely decomposed to individual molecules. For instance, ΔG^0 is obtained by

$$\Delta G^0 = G(\text{Li}^+ - \text{PC}_x)^0 - xG(\text{PC})^0 - G(\text{Li}^+)^0 \qquad (1)$$

where $G(\text{species})^0$ stands for the standard Gibbs energy for the concerning species obtained by the procedure in Appendix. ΔH^0 and ΔS^0 are obtained in the same manner described in Eq. 1. It is clearly seen from Table 3 that the Gibbs energy change favors the formation of Li$^+$–PC$_4$ complex, again confirming it is the most plausible solvated complex also from the thermochemical viewpoint.

Desolvation on the modeled carbon electrode

From the above results, the most favorable solvated complex is Li$^+$–PC$_4$ and its tetrahedral-like configuration is shown in Fig. 4. The largest diameter of this complex is

Table 1 Net charge of a Li$^+$ ion solvated with PC molecules with interatomic distances between Li and carbonyl O

	Average distance of Li–carbonyl O/pm	Maximum distance of Li–carbonyl O/pm	Atomic net charge of Li	Atomic net charge of carbonyl O
Li$^+$–PC	172.8	172.8	+0.83	−0.60
Li$^+$–PC$_2$	177.4	177.4	+0.69	−0.55
Li$^+$–PC$_3$	184.2	184.2	+0.60	−0.50
Li$^+$–PC$_4$	192.1	192.1	+0.50	−0.46
Li$^+$–PC$_5$	206.0	224.3	+0.41	−0.45 (av)
Li$^+$–PC$_6$	219.0	235.4	+0.36	−0.43 (av)

Table 2 Bond-order analysis based on the atom–atom overlap-weighted NAOs

	Bond order between Li and carbonyl O (in order of magnitude)					
Li$^+$–PC	0.1414					
Li$^+$–PC$_2$	0.1472	0.1472				
Li$^+$–PC$_3$	0.1332	0.1331	0.1330			
Li$^+$–PC$_4$	0.1185	0.1185	0.1184	0.1184		
Li$^+$–PC$_5$	0.1044	0.1012	0.1011	0.0857	0.0695	
Li$^+$–PC$_6$	0.0803	0.0803	0.0802	0.0794	0.0605	0.0583

**Table 3** Standard enthalpy, entropy, and Gibbs energy change upon solvation (at 298.15 K and 101325 Pa)

	Li$^+$–PC	Li$^+$–PC$_2$	Li$^+$–PC$_3$	Li$^+$–PC$_4$	Li$^+$–PC$_5$	Li$^+$–PC$_6$
ΔH^0	−241.17	−423.46	−532.62	−598.06	−624.00	−646.60
ΔS^0	−96.78	−215.39	−317.02	−461.87	−654.71	−823.08
ΔG^0	−212.34	−359.24	−438.11	−460.37	−428.78	−401.20

ΔH^0 and ΔG^0 are shown in kJ mol^{-1} and ΔS^0 in J K^{-1} mol^{-1}

1426 pm, whereas that of a PC molecule is 484 pm. The size of Li$^+$–PC$_4$ complex thus obtained is rather large when compared with the interlayer distance of graphite (335.4 pm) and general amorphous carbon material (370–410 pm) [11], and with the diameter of micropores in the porous amorphous carbon (ca. 500 pm) [12] which are often used as the negative electrode in the lithium-ion battery. Hence, it is rather natural to consider that liberation of some or all the PC molecules, i.e., desolvation should occur when the Li$^+$–PC$_4$ complex is doped into carbon materials as well as enters into the micropores, generally forming the surface of carbon electrode.

At the adsorption mode onto an ovalene wall it has been found that the Li$^+$–PC$_4$ complex tends to be decomposed and that the Li$^+$–PC$_3$ complex keeps rather far away from the ovalene plane with the distance between Li$^+$ and the wall of 362.4 pm. The latter fact suggests that the Li$^+$–PC$_3$ complex almost cannot be adsorbed onto the carbon wall. As seen in Fig. 5a, at least Li$^+$–PC complex can be adsorbed on the carbon wall. The energy potential becomes
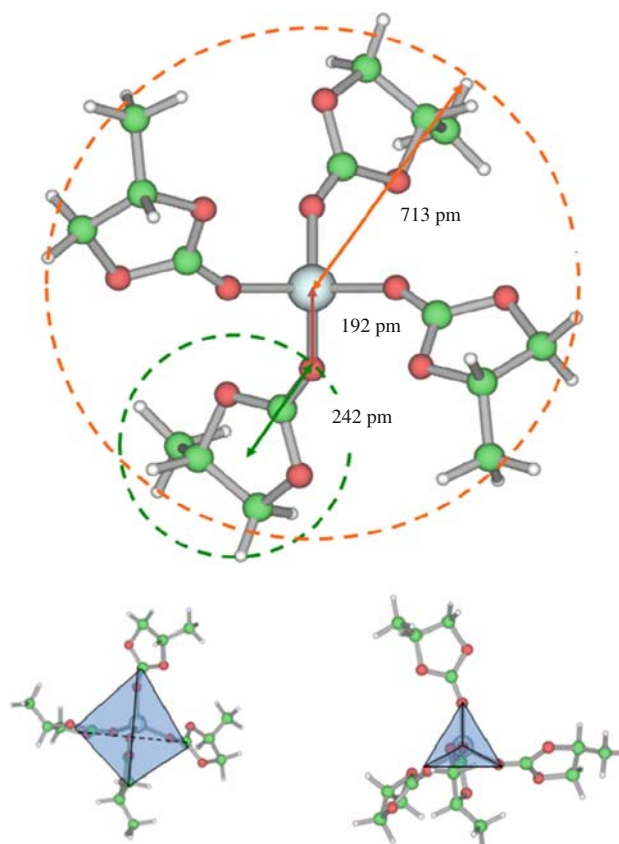
Fig. 4 Optimized configuration of Li$^+$–PC$_4$, forming an approximately tetrahedral structure for the four Li–carbonyl O bonds as seen in the *bottom pictures*

minimum at the Li$^+$ and the wall distance of 217.2 pm. The Li-carbonyl O distance is calculated to be 172.8 pm being the same as that without the wall (see Table 1). On the other hand, Fig. 5b for Li$^+$–PC$_2$ complex suggests that its structure is rather distorted.

When the solvated Li$^+$–PC$_4$ complex is inserted into the two walls, the complex configuration will be considerably distorted there as seen in Fig. 6a, since the distance between the walls (600 pm) is too tight. Hence, the Li–carbonyl O distances become 190.3, 192.2, 208.3, and 235.9 pm, strongly suggesting that two PC molecules are to
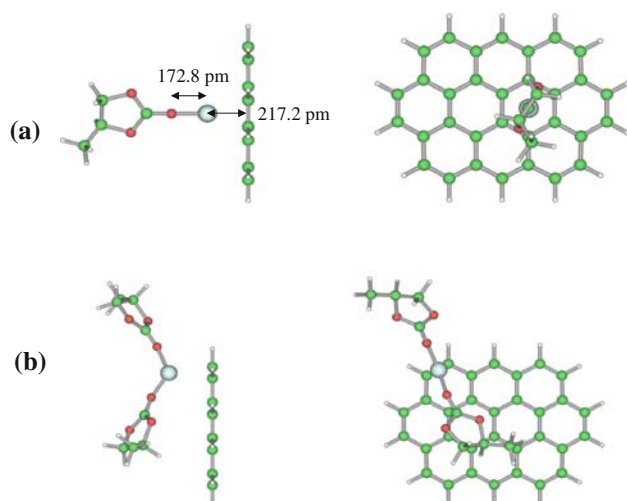
Fig. 5 Adsorption mode of the solvated Li^+-ion complex onto a wall model: *top view* (*left*) and *side view* (*right*). **a** Li^+–PC and **b** Li^+–PC_2. See Fig. 2a with respect to the molecular structure of ovalene employed as the wall model
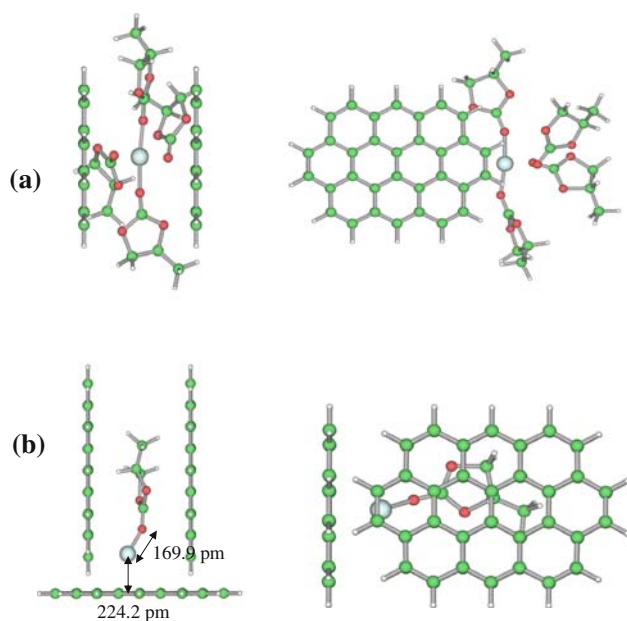

Fig. 6 a Insertion mode of Li^+–PC_4 between two-wall model: *top view* (*left*) and *side view* (*right*). **b** Adsorption mode of a Li^+–PC inside a micropore model: *top view* (*left*) and *side view* (*right*). See Fig. 2 with respect to the configurations of the two-wall and the micropore models

be desolvated from the complex. Note that the supermolecule configuration including this "Li^+–PC_4 complex" and the two walls in Fig. 6a is still in the potential minimum.

The energy potential calculation for the adsorption mode into the micropore model adopt only Li^+–PC complex can "enter" the micropore in the energetically stable manner. The energy potential becomes minimum at the Li^+ and the

wall distance is calculated to be 224.2 pm being slightly larger when compared with that for the adsorption mode onto a wall in Fig. 5a. It is of somewhat interest that Li–carbonyl O distance becomes reduced to 169.9 pm, which is even shorter than that of the single Li^+–PC complex (see Table 1). This shrinkage again suggests that Li^+–PC can remain inside the carbon micropore.

Conclusions

In this study, we have obtained two major results:

(i) Four PC molecules is the "magic number" for the solvated Li^+–PC_x complex in the PC solution. This number is in agreement with the Li^+–EC_x complex previously studied.

(ii) When this Li^+–PC_x complex approaches and is adsorbed on the carbon electrode surface, it is highly possible that desolvation occurs but at least one PC molecule can remain as the Li^+–PC complex adsorbed onto the carbon wall or inside the micropore.

References

1. Linden D. Handbook of batteries. Part II. 2nd ed. New York: McGraw-Hill; 1995.
2. Hyodo S, Okabayashi K. Raman intensity study of local structure in non-aqueous electrolyte solutions—I. Cation-solvent interaction in $LiClO_4$/ethylene carbonate. Electrochim Acta. 1989; 34(11):1551–6.
3. Hyodo S, Okabayashi K. Raman intensity study of local structure in non-aqueous electrolyte solutions—II. Cation-solvent interaction in mixed solvent systems and selective solvation. Electrochim Acta. 1989;34(11):1557–61.
4. Yanase S, Oi T. Solvation of lithium ion in organic electrolyte solutions and its isotopic reduced partition function ratios studied by ab initio molecular orbital method. J Nucl Sci Technol. 2002;39(10):1060–4.
5. Jarek RL, Miles TD, Trester ML, Denson SC, Shin SK. Solvation of Li^+ by acetone, THF, and diethyl ether in the gas phase and the ion-molecule association mechanism. J Phys Chem A. 2000; 104(11):2230–7.
6. Spångberg D, Hermansson K. The solvation of Li^+ and Na^+ in acetonitrile from ab initio-derived many-body ion-solvent potentials. Chem Phys. 2004;300(1–3):165–76.
7. Arai J, Katayama H, Akahoshi H. Binary mixed solvent electrolytes containing trifluoropropylene carbonate for lithium secondary batteries. J Electrochem Soc. 2002;149(2):A217–26.
8. Reed AE, Curtiss LA, Weinhold F. Intermolecular interactions from a natural bond orbital, donor–acceptor viewpoint. Chem Rev. 1988;88(6):899–926.
9. Frisch MJ, et al. Gaussian 03. Revision E.01. Wallingford: Gaussian Inc; 2004.
10. Del Piero S, Melchior A, Menotti D, Tolazzi M, Døssing A. Solvent effect on the thermodynamics of Ag(I) coordination to

tripodal polypyridine ligands. J Therm Anal Calorim 2009;
97(3):845–51.

11. Tanaka K, Ueda M, Koike T, Yamabe T, Yata S. X-ray dif-
fraction studies of pristine and heavily-doped polyacenic mate-
rials. Synth Met. 1988;25(3):265–75.

12. Yata S, Hato Y, Sakurai K, Satake H, Mukai K, Tanaka K, et al.
Studies of porous polyacenic semiconductors toward application
I. Preparation and structural analysis. Synth Met. 1990;
38(2):169–75.